Rare Decays Including Penguins

SLAC-PUB-10260

Gerald Eigen

University of Bergen, Bergen, Norway

For the BABAR Collaboration

Abstract

We present a preliminary measurement of the exclusive charmless semileptonic B decay, $B \to \rho\ell\nu$, and the extraction of the CKM parameter V_{ub}. In a data sample of 55×10^6 $B\bar{B}$ events we measure a branching fraction of $\mathcal{B}(B \to \rho\ell\nu) = (3.39 \pm 0.44_{stat} \pm 0.52_{sys} \pm 0.60_{th}) \times 10^{-4}$ yielding $|V_{ub}| = (3.69 \pm 0.23_{stat} \pm 0.27_{sys}{}^{+0.40}_{-0.59th}) \times 10^{-3}$. Next, we report on a preliminary study of the radiative penguin modes $B \to K\ell^+\ell^-$ and $B \to K^*\ell^+\ell^-$. In a data sample of 84×10^6 $B\bar{B}$ events we observe a significant signal (4.4σ) in $B \to K\ell^+\ell^-$, yielding a branching fraction of $\mathcal{B}(B \to K\ell^+\ell^-) = (0.78^{+0.24+0.11}_{-0.20-0.18}) \times 10^{-6}$. In $B \to K^*\ell^+\ell^-$ the observed yield is not yet significant (2.8σ), yielding an upper limit of the branching fraction of $\mathcal{B}(B \to K^*\ell^+\ell^-) < 3.0 \times 10^{-6}$ @ 90% confidence level. Finally, we summarize preliminary results of searches for $B \to \rho(\omega)\gamma$, $B^+ \to K^+\nu\bar{\nu}$ and $B^0 \to \ell^+\ell^-$.

Presented at Beauty 2002:
8th International Conference on B Physics at Hadron Machines,
Santiago de Compostela, Spain, 6/17/2002 - 6/21/2002

Work supported in part by Department of Energy contract DE-AC03-76SF00515.
Stanford Linear Accelerator Center, Stanford University, Stanford, CA 94309

1 Introduction

With the rapid successful startup of asymmetric B factories huge samples of B mesons have become available, approaching $10^8 B\bar{B}$ events. Such high-statistics data samples allow us to perform precision measurements of observables such as CP violating asymmetries, improve the precision on present branching fractions such as $b \to u$ transitions or to explore new domains of rare decays with branching fractions of the order of $10^{-5} - 10^{-7}$. The present BABAR measurement of $\sin 2\beta = 0.741 \pm 0.067 \pm 0.033$ [1], for example, already reaches a precision of $\leq 10\%$. The determination of $|V_{ub}|$ from $B \to \rho\ell\nu$ is accomplished with an experimental error below 10%. In radiative penguin decays such as $B \to K\ell^+\ell^-$ first signals appear. In this report we focus on new preliminary BABAR results of the charmless exclusive semileptonic decay $B \to \rho e\nu$, present a preliminary study of the electroweak penguin decays $B \to K^{(*)}\ell^+\ell^-$ and summarize the status of searches for $b \to d$ radiative penguin modes, $B \to \rho(\omega)\gamma$, the exclusive weak decay $B^+ \to K^+\nu\bar{\nu}$ and the highly-suppressed weak decays $B \to \ell^+\ell^-$.

2 Branching Fraction Measurement of the Exclusive Decay $\mathbf{B^0 \to \rho^- e^+ \nu}$ and Determination of $|\mathbf{V_{ub}}|$

Charmless semileptonic B decays provide the best technique for measuring V_{ub}, one of the smallest and least known elements of the Cabibbo-Kobayashi-Maskawa (CKM) matrix, since leptonic and hadronic currents factorize in this tree-level process and, therefore, uncertainties arising from QCD corrections are reduced. The experimental challenge, however, consists of suppressing large backgrounds from charmed semileptonic decays and $q\bar{q}$ continuum. Thus, the first V_{ub} measurements were obtained from the lepton endpoint spectrum above the $B \to X_c\ell\nu$ limit [2]. The model dependence, however, is rather large ($\sim 20\%$) as only $\sim 10\%$ of the $B \to X_u\ell\nu$ lepton spectrum is selected. Another strategy focuses on exclusive decays, such as $B \to \rho\ell\nu$ [3]. Here the extraction of V_{ub} is affected by the model dependence of hadronic form factors yielding a theoretical uncertainty of $\sim 15\%$. The smallest model dependence in the determination of V_{ub} ($\sim 10\%$) may obtained from an inclusive analysis that is performed in a region of hadronic mass below the D meson and at high $q^2 = (p_\ell + p_\nu)^2$. This recently proposed strategy [4] also allows to reduce the $B \to X_c\ell\nu$ background substantially.

Following a strategy developed by CLEO [3], we have analyzed exclusive charmless semileptonic decays $B \to M_u e^\pm \nu$ in BABAR, where M_u denotes a $\pi^0, \rho^0, \omega, \pi^\mp$ or $\rho^\mp$ in the final state [5]. We perform the analysis in two lepton momentum ranges $2.0 \leq p_e \leq 2.3$ GeV/c (LOLEP) and $2.3 \leq p_e \leq 2.7$ GeV/c (HILEP), containing each around 30% of the signal. The $B \to X_c e\nu$ background which dominates the LOLEP region is significantly reduced in the HILEP region. The other discriminating kinematic variables are the invariant mass of the hadronic two-pion or three-pion systems, m_{had}, and the difference of the B meson energy and the beam energy in the center-of-mass (CM) frame, $\Delta E^* = E^*_B - E^*_{beam}$, where the B meson energy is reconstructed from the energies of the hadronic system, the electron, and the missing momentum in the event, $E^*_B = E^*_{had} + E^*_e + |\vec{p}^*_{miss}|$. The original analysis was updated for the summer with a data sample consisting of an integrated luminosity of 50.5 fb^{-1} (*i.e.* 55.2×10^6 $B\bar{B}$ events) collected at the $\Upsilon(4S)$ resonance and 8.7 fb^{-1} 40 MeV below the $\Upsilon(4S)$. The event selection is optimized for ρ final states but all five modes are included to account for cross-feeds.

Candidate events with at least five charged tracks or four charged tracks plus five photons satisfying standard charged-track and photon quality requirements, must have one well-identified electron, which is selected with the help of a likelihood-based estimator. The most significant variable is the ratio of calorimeter energy to track momentum. The selection yields an efficiency of $\sim$ 90% for a pion misidentification probability of $\leq 0.1\%$. Electrons from J/ψ decays ($3.0 < M_{e^+e^-} < 3.14$ GeV/c^2) and photon conversions ($M_{e^+e^-} < 30$ MeV/c^2) are removed explicitly. Charged tracks forming the hadronic system must be inconsistent with a kaon hypothesis. At least one π forming a ρ must have a momentum greater 0.4 GeV/c. A π^0 candidate must have a two-photon invariant mass of $^{+10}_{-15}$ MeV/c^2 around the nominal π^0 mass. For an ω candidate the three-pion invariant mass has to be within ± 80 MeV/c^2 of the nominal ω mass. Requiring the ratio of second-to-zeroth Fox-Wolfram moments [11] to satisfy $R_2 < 0.4$, removes 55% of the $e^+e^- \to q\bar{q}$ continuum background while retaining an 85% efficiency for signal events.

We further exploit kinematic constraints to remove backgrounds from $B \to X_c e\nu$ and $q\bar{q}$ continuum. Denoting the observed system consisting of the e^+ and the hadron (ρ, ω, π) by Y the constraints in the CM frame, $E^*_B = E^*_{beam}$ and $m^2_\nu = (p^*_B - p^*_Y)^2 = 0$, provide a determination of the angle between the B meson and the hadronic system, θ_{BY}, up to a two-fold ambiguity. While signal events are constrained to the physical region ($|\cos\theta_{BY}| < 1$), background also falls into the non-physical region. Thus, taking into account effects of the detector resolution we require $|\cos\theta_{BY}| < 1.1$, which is almost 100% efficient for signal events but rejects $> 60\%$ of the $B \to X_c e\nu$ and 80% of the $q\bar{q}$ continuum backgrounds. Since one solution for the predicted ν direction ($\vec{p}^{*min}_\nu$) has to be consistent with the direction of $\vec{p}^*_{miss}$, we require the angle θ_{min} between $\vec{p}^*_{miss}$ and $\vec{p}^{*min}_\nu$ in the plane spanned by $\vec{p}^*_Y$ and $\vec{p}^*_\nu$ to satisfy $0.8 < \cos\Delta\theta_{min} \leq 1.0$. In addition, we require the angle between $\vec{p}^*_{miss}$ and the beam axis to satisfy $|\cos\theta_{miss}| < 0.9$, which removes events with missing momentum near the beam axis. To further suppress $q\bar{q}$ continuum background we use the output of a neural network that is based on 14 event-shape variables including the energy flow in nine cones around $e^\pm$ direction and the thrust angle θ_T. In the HILEP region the $q\bar{q}$ continuum background rejection is increased to $> 90\%$ while retaining a signal efficiency of 60%. To reduce combinatorial background we select only one combination per event, which is chosen to be that where the reconstructed total momentum $|\vec{p}^*_Y + \vec{p}^*_{miss}|$ is closest to $|\vec{p}^*_B|$. Further analysis details are given in [5].

Signal yields are extracted from an extended binned maximum likelihood fit in the ΔE^*-m_{had} plane, performed simultaneously in the two lepton-energy regions. The fit includes contributions from the five signal channels, other $B \to X_u e\nu$ modes, $B \to X_c e\nu$ modes, $q\bar{q}$ continuum and decays with a misidentified electron. For the $B \to \pi e\nu$ modes only ΔE^* is used as a fit variable. The shapes of the ΔE^* and m_{had} distributions for signal and backgrounds are obtained from Monte Carlo simulations. To reduce the number of

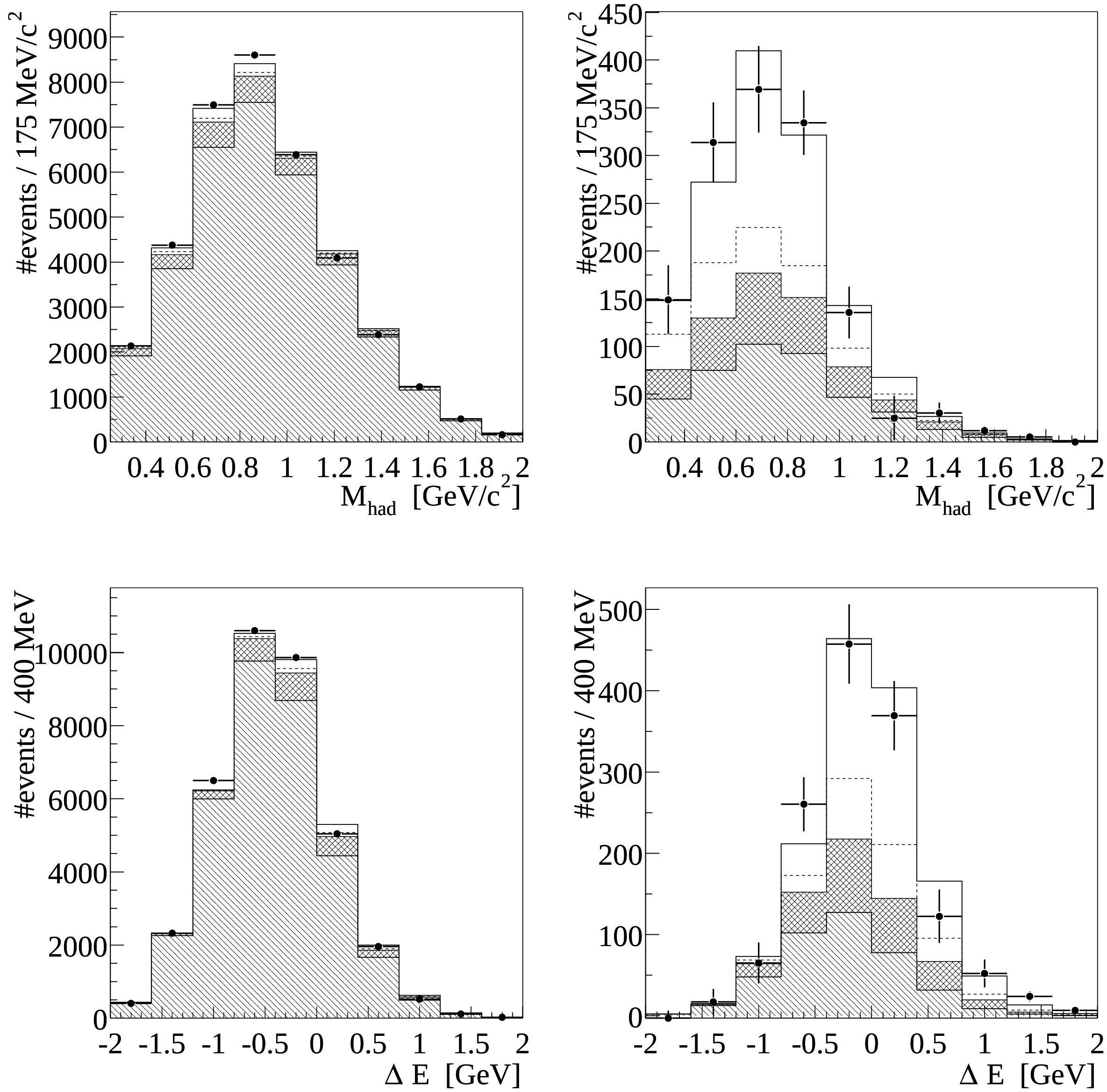

Figure 1: Continuum-subtracted $M_{\pi\pi}$ and ΔE^* projections in the LOLEP (left) and HILEP (right) electron energy regions for $B^+ \to \rho^- e^+ \nu$ obtained from a fit to the ISGW2 model [6]. The points with error bars represent the data. Unhatched histograms show the signal contribution, dashed histograms the cross-feed components, double-hatched regions other $B \to X_u e\nu$ background modes, and single-hatched regions the $B \to X_c e\nu$ and other backgrounds.

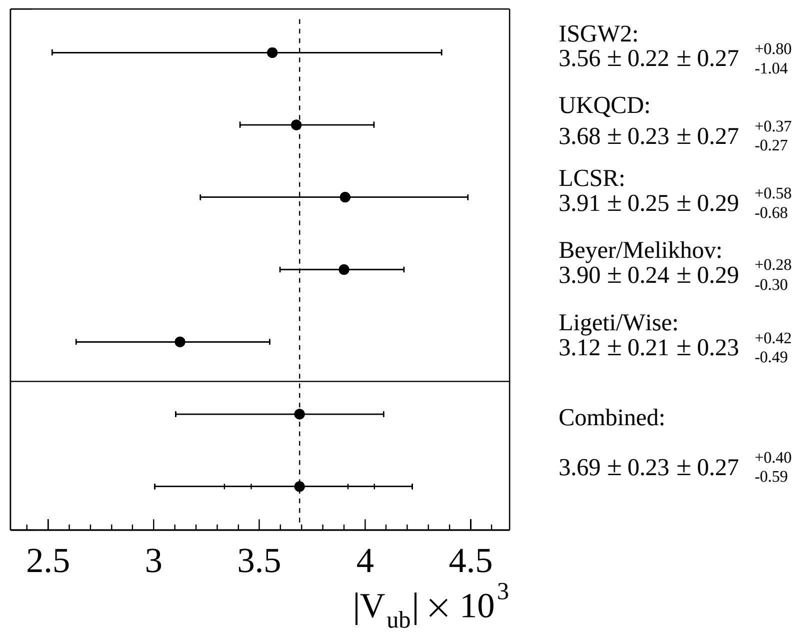

Figure 2: Values of $|V_{ub}|$ extracted from fits to five form-factor models [6, 7, 8, 9, 10]. For each model only the theoretical uncertainty is plotted. The combined central value is determined by weighting the individual central values by their theoretical uncertainty. The theoretical uncertainty of the combined result is taken as one half of the full spread including errors. The individual results are listed on the right-hand side. The errors denote statistical, systematic, and theoretical uncertainties, respectively. For the combined results these errors are also shown after adding them successively in quadrature.

fit parameters we constrain the relative normalizations of vector and pseudo-scalar modes separately, employing isospin symmetry and quark models relations, $\Gamma(B^0 \to \rho^- e^+\nu) = 2\Gamma(B^+ \to \rho^0 e^+\nu)$, $\Gamma(B^+ \to \rho^0 e^+\nu) = \Gamma(B^+ \to \omega e^+\nu)$, and $\Gamma(B^0 \to \pi^- e^+\nu) = 2\Gamma(B^+ \to \pi^0 e^+\nu)$. The fit has nine free parameters, consisting of the branching fractions $\mathcal{B}(B^0 \to \rho^- e^+\nu)$ and $\mathcal{B}(B^0 \to \pi^- e^+\nu)$, scale factors for the $B \to X_u e\nu$ background in the two lepton-energy regions, and scale factors for the $B \to X_c e\nu$ background in each signal mode. Since the shape of the kinematic distributions is model dependent we have used five different form-factor models for the signal modes in the fits [6, 7, 8, 9, 10]. The ΔE^* and m_{had} projection for the LOLEP and HILEP regions obtained from the fit in the ISGW2 model [6] are displayed in Figure 1.

The maximum likelihood fits to the ISGW2 model yield 324 ± 40 $B^+ \to \rho^0 e^+\nu$ and 510 ± 63 $B^0 \to \rho^- e^+\nu$ candidates in the HILEP region, where the selection efficiencies are determined to be 4.2% and 3.3%, respectively. Since $B^0 \to \rho^- e^+\nu$ has the highest sensitivity, it is used for measuring the branching fraction and for extracting $|V_{ub}|$. To account for the model dependence we determine a branching fraction for each of the five

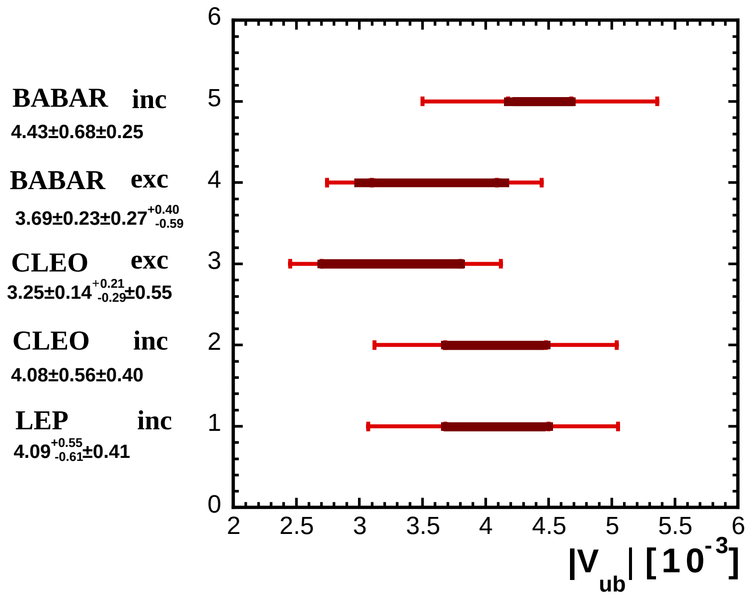

Figure 3: Comparison of $|V_{ub}|$ measurements from BABAR [5, 14], CLEO [2, 13] and LEP [15]. For exclusive (inclusive) results statistical, systematic and theoretical (total experimental and theoretical) errors are quoted. Thick bars show the spread due to theoretical uncertainties, while thin error bars show pure experimental errors.

form-factor models. An unweighted mean of the individual results yields the combined branching fraction of $\mathcal{B}(B^0 \to \rho^- e^+ \nu) = (3.39 \pm 0.44_{stat} \pm 0.52_{sys} \pm 0.60_{th}) \times 10^{-4}$, where the errors denote statistical, systematic and theoretical uncertainties, respectively. The largest contributions of the 15.5% systematic error on the branching fraction arise from uncertainties of the non-resonant $B \to X_u e \nu$ background component ($\pm 9\%$), data selection ($\pm 6\%$), fit method ($^{+4}_{-6}\%$), resonant $B \to X_u e \nu$ backgrounds ($^{+6}_{-4}\%$), tracking efficiency ($\pm 5\%$) and the photon efficiency ($\pm 5\%$).

The CKM matrix element $|V_{ub}|$ is extracted from the measured branching fraction using

$$| V_{ub} |= \sqrt{\frac{\mathcal{B}(B^0 \to \rho^- e^+ \nu)}{\tilde{\Gamma}_{thy} \tau_{B^0}}}, \tag{1}$$

where $\tilde{\Gamma}_{thy}$ is the reduced rate calculated in a form-factor model and $\tau_{B^0} = (1.548 \pm 0.032)$ ps is the B^0 lifetime [12]. The uncertainties on $\tilde{\Gamma}_{thy}$ range between 15% [8] and 50% [6]. Figure 2 shows the individual values of $|V_{ub}|$ extracted from each of the five form-factor models. The combined result, which is taken as the mean of the five central values weighted with each theoretical uncertainty, yields $|V_{ub}| = (3.69 \pm 0.23_{stat} \pm 0.27_{sys}{}^{+0.40}_{-0.59 th}) \times 10^{-3}$. The theoretical uncertainty is taken to be one half of the full spread of all fit results including theoretical errors. Note that the theoretical uncertainty in $|V_{ub}|$ enters in three places, the selection efficiency, the branching fraction and $\tilde{\Gamma}_{thy}$. The theoretical uncertainty specifies a range of $|V_{ub}| = (3.1 - 4.09) \times 10^{-3}$. Figure 3 shows a comparison of present $|V_{ub}|$ measurements. To emphasize that the theoretical uncertainties are non-probabilistic errors we plot the spread of the theoretical uncertainty rather than a central value. The additional error bars denote experimental errors added in quadrature. Within the theoretical uncertainty alone our measurement is consistent with the exclusive CLEO result and inclusive results from CLEO [13], BABAR [14] and a LEP average over all experiments [15].

3 Study of $\mathbf{B \to K\ell^+\ell^-}$ and $\mathbf{B \to K^*\ell^+\ell^-}$ Final States

The electroweak decays $B \to K\ell^+\ell^-$ and $B \to K^*\ell^+\ell^-$ are flavor-changing neutral current processes like $B \to K^*\gamma$, which are forbidden in the Standard Model (SM) at tree level. They proceed via an electromagnetic penguin, a Z^0 penguin and a weak box diagram as shown in Figure 4. The branching fractions predicted in SM are of the order of $10^{-7} - 10^{-6}$ [16, 28, 17]. The calculations are based on an effective Hamiltonian which factorizes the perturbatively calculable short-distance contributions parameterized in terms of scale-dependent Wilson coefficients from the non-perturbative long distance effects expressed by local dimension-six four-quark operators. Due to operator mixing in next-to-leading order perturbation theory one obtains effective scale-dependent Wilson coefficients, $C_7^{eff}(\mu_b), C_9^{eff}(\mu_b)$, and $C_{10}^{eff}(\mu_b)$, where μ_b represents the mass scale. For comparison, in $b \to s\gamma$ modes only $C_7^{eff}(\mu_b)$ is present. New Physics processes are expected to contribute via additional loop and box diagrams. For example, particles in the loop can be replaced with their supersymmetric partners or the W boson can be exchanged with a charged Higgs boson. The New Physics contributions interfere with the SM contributions, modifying the Wilson coefficients. For example, the destructive interference between $C_7^{eff}(\mu_b)$ and $C_9^{eff}(\mu_b)$ in SM may be reduced or even turned into constructive interference by new contributions to C_7^{eff}, thus typically leading to enhanced branching fractions. Recently, the model by Ali *et al.* [16] updated their SM branching fraction predictions for these modes, yielding $\mathcal{B}(B \to K\ell^+\ell^-) = (0.35 \pm 0.12) \times 10^{-6}$ for both e^+e^- and $\mu^+\mu^-$ modes, $\mathcal{B}(B \to K^*e^+e^-) = (1.58 \pm 0.49) \times 10^{-6}$, and $\mathcal{B}(B \to K^*\mu^+\mu^-) = (1.19 \pm 0.39) \times 10^{-6}$. In supersymmetric models branching fractions may be enhanced by more than a factor of two [16].

The original BABAR [18] analysis has been updated for the summer and is based on a data sample consisting of 77.8 fb^{-1} that was recorded at the $\Upsilon(4S)$ resonance [*i.e.* $(84.4 \pm 0.9) \times 10^6$ $B\bar{B}$ events] and 9.6 fb^{-1} that was taken 40 MeV below $\Upsilon(4S)$ peak. Eight exclusive final states have been studied consisting of a K^+, K_S^0, K^{*0} or K^{*+} recoiling against e^+e^- or $\mu^+\mu^-$, where the K^* and K_S^0 were reconstructed only in modes containing charged pions. The discriminating variables are the beam-energy substituted mass $m_{ES} = \sqrt{(E^*)^2_{beam} - (\vec{p}^*_B)^2}$ and ΔE^*, where the B meson is reconstructed from all observed daughter particles. The $\Delta E - m_{ES}$ plane is divided into three regions, the signal region ($\pm 3\sigma$ boxes around signal), the fit region ($m_{ES} > 5.2$ GeV/c^2, $|\Delta E^*| < 250$ MeV) and the large sideband ($m_{ES} > 5.0$ GeV/c^2, $|\Delta E^*| < 500$ MeV). The fit region and

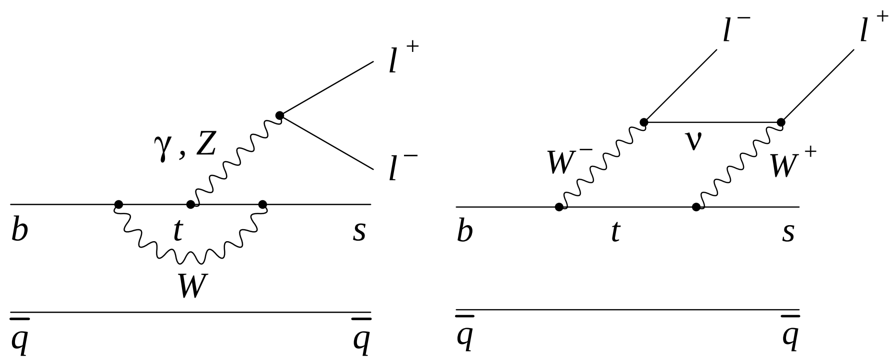

Figure 4: Lowest-order diagrams for $B \to K^{(*)}\ell^+\ell^-$ in SM.

the signal region are concealed during the event selection process. Candidate events are required to have at least four charged tracks with $R_2 < 0.5$ of which two tracks are identified as oppositely charged leptons with momenta $p^*_\ell > 0.5$ (1.0) GeV/c for $e^\pm$ ($\mu^\pm$). An e^+e^- pair that is consistent with a photon conversion is vetoed. Pions have to be inconsistent with a kaon hypothesis and charged kaons have to be identified as such with strict criteria. The $K\pi$ invariant mass has to lie within 75 MeV/c^2 of the nominal K^* mass. K^0_S candidates must have a vertex displaced by > 1mm from the primary vertex and a $\pi^+\pi^-$ invariant mass within ± 9.3 MeV/c^2 of the nominal K^0_S mass.

Specific criteria have been developed to suppress different sources of background. Event shape variables are used to reject $q\bar{q}$ continuum background. We combine R_2 [11], the B decay angle (θ_B), the thrust angle (θ_T) of the B candidate and the rest of the event, and the invariant mass of the $K\ell$ system into a Fisher discriminant [19], which is optimized separately for each decay channel. Combinatorial background from $B\bar{B}$ events is reduced by a likelihood ratio that combines candidate B and dilepton vertex probabilities, the significance of dilepton separation along the beam direction, the B decay angle and the missing energy, E^*_{miss}, in the event in the CM frame. Since events with semileptonic decays have a significant fraction of unobserved energy due to ν's, E^*_{miss} provides the strongest discrimination against $B\bar{B}$ background. The exclusive modes $B \to J/\psi(\to \ell^+\ell^-)K^{(*)}$ and $B \to \psi(2S)(\to \ell^+\ell^-)K^{(*)}$ have identical topologies to the signal modes. To remove this background, dilepton masses around the J/ψ and $\psi(2S)$ are vetoed (vertical bands in Figure 5). This veto, however, misses events where due to photon radiation or track mismeasurement both ΔE^* and $m_{\ell^+\ell^-}$ are reduced such that they fall outside the vertical band. To remove these events both in the signal and sideband regions candidates are rejected that fall into the hatched regions in the $\Delta E^* - m_{\ell^+\ell^-}$ plane shown in Figure 5. In $\mu^+\mu^-$ final states events are vetoed that are consistent with $B \to D(\to K^{(*)}\pi)\pi$ when particle hypotheses are interchanged. In addition, events are rejected, if dilepton masses are consistent with a J/ψ or $\psi(2S)$ after swapping kaon and lepton identifications. Other peaking background are found to be small. For each final state at most one combination

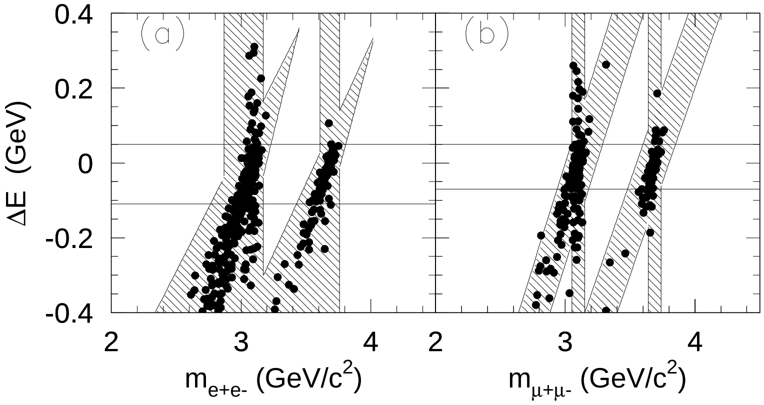

Figure 5: Charmonium veto (hatched regions) in the $\Delta E^* - m_{\ell^+\ell^-}$ plane for a) $B \to K^{(*)}e^+e^-$ and b) $B \to K^{(*)}\mu^+\mu^-$. The dots represent simulations for $B \to J/\psi(\to \ell^+\ell^-)K$ and $B \to \psi(2S)(\to \ell^+\ell^-)K$.

is selected, which in case of multiple candidates is that with the largest number of hits in the drift chamber and silicon vertex detector. Further analysis details are given in [18].

The selection criteria have been optimized on simulated signal and background events as well as off-resonance data and events in the large sideband. Signal Monte Carlo samples provide efficiencies and allow to study peaking backgrounds. In order to crosscheck the Monte Carlo with data, different control samples have been studied. Exclusive charmonium decays provide a direct comparison in a restricted $m_{\ell^+\ell^-}$ region, yielding an agreement of the data with the Monte Carlo simulations of $(101.5 \pm 1.9)\%$ after summing over eight final states. Exclusive $B \to D\pi$ decays and inclusive charmonium modes $B \to J/\psi X_s$ allow to investigate peaking backgrounds, while $e^\pm\mu^\mp K^{(*)}$ combinations and events in the large side bands provides estimates on combinatorial backgrounds. The signal in each mode is extracted from a two-dimensional fit in the $\Delta E^* - m_{ES}$ plane. The signal shapes are obtained from Monte Carlo samples with fine-tuning on the exclusive charmonium modes. To account for effects of radiation and a correlation between ΔE^* and m_{ES} a product of Crystal Ball functions is used [20]. The combinatorial background is parameterized by an ARGUS function [21]. Both the normalization and the shape parameters are left free in the fit. Figure 6 shows the resulting m_{ES} projections in each channel with fits superimposed. A significant signal with a yield of $14.4^{+5.0}_{-4.2}$ events is only observed in the $B^+ \to K^+e^+e^-$. The selection efficiency is 17.5%, yielding a branching fraction of

$$\mathcal{B}(B^+ \to K^+e^+e^-) = (0.98^{+0.34+0.16}_{-0.28-0.22}) \times 10^{-6}. \tag{2}$$

The event yields observed in the $B \to K^*\ell^+\ell^-$ modes are not significant. The largest yield seen in $B^0 \to K^{*0}e^+e^-$ consists of $10.6^{+5.2}_{-4.3}$ events.

The multiplicative systematic errors range from $7\% - 8\%$ in $K^+\ell^+\ell^-$ and $7\% - 11\%$

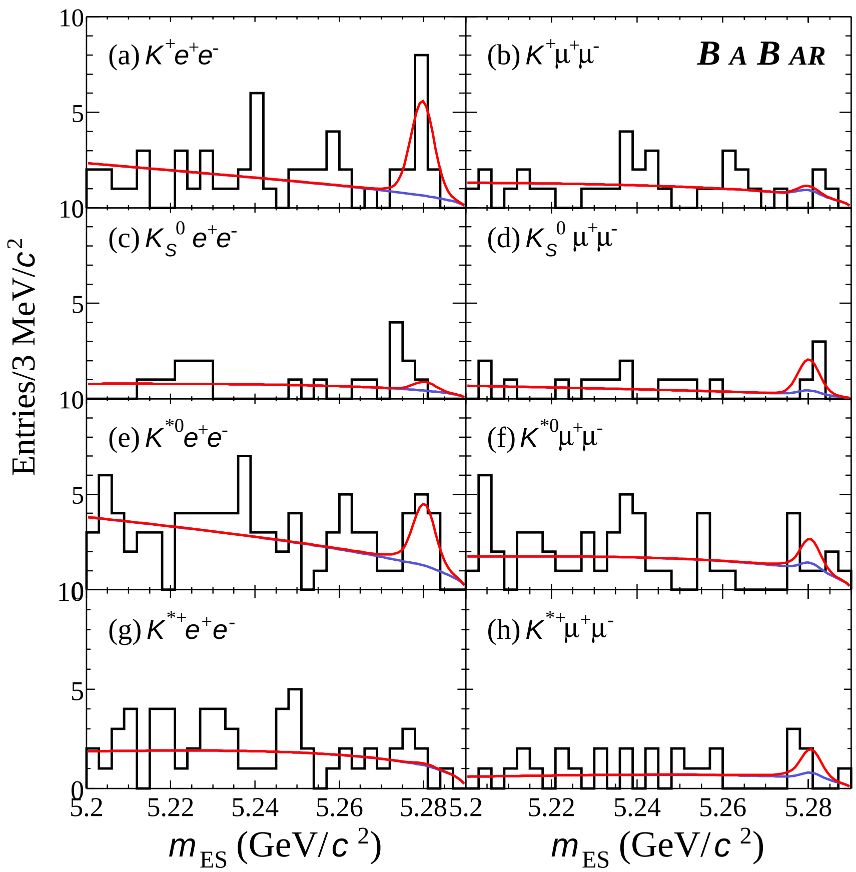

Figure 6: The m_{ES} projections of the individual fits in the ΔE^* regions $-0.11 \leq \Delta E^* \leq 0.05$ GeV for e^+e^- and $-0.07 \leq \Delta E^* \leq 0.05$ GeV for $\mu^+\mu^-$ modes. Histograms show data and solid curves represent fits.

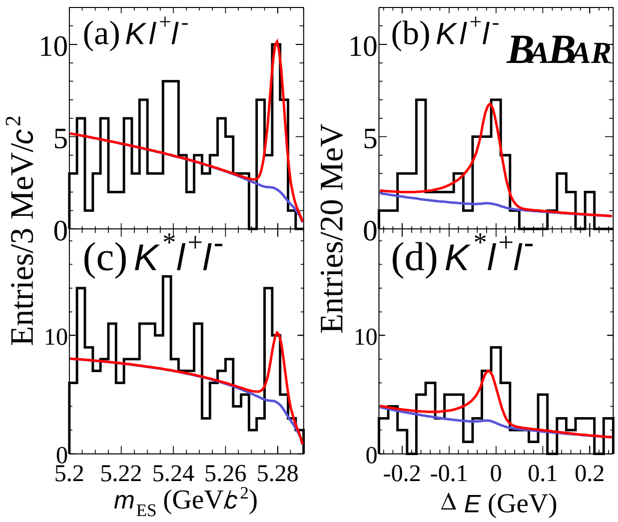

Figure 7: Summed m_{ES} and ΔE^* projections of the combined fits for all four $B \to K\ell^+\ell^-$ and four $B \to K^*\ell^+\ell^-$ modes.

in $K^*\ell^+\ell^-$ modes. The largest contributions come from the model dependence ($4\% - 7\%$), electron/muon identification ($2.7/2.0\%$), kaon/pion identification ($2.0\% - 4.0\%$), K_S^0 efficiency (3.2%), $B\bar{B}$ likelihood ratio (2.5%), tracking efficiency for hadrons ($1.3\%-3.9\%$), and tracking efficiency for leptons (1.6%). Contributions from Fisher discriminant, Monte Carlo statistics and $B\bar{B}$ counting are small ($< 2\%$). In addition, additive systematic errors result from the signal yields in the fit and include uncertainties in signal shapes, in background shapes and in the amount of peaking backgrounds. The m_{ES} and ΔE^* distributions of combined $B \to K\ell^+\ell^-$ and $B \to K^*\ell^+\ell^-$ modes are displayed in Figure 7. A significant signal is observed in $B \to K\ell^+\ell^-$. The significance based purely on statistical errors is 5.6σ. When systematic uncertainties are included the significance drops to 4.4σ. The branching fraction of the combined $B \to K\ell^+\ell^-$ modes is measured to be

$$\mathcal{B}(B \to K\ell^+\ell^-) = (0.78^{+0.24+0.11}_{-0.20-0.18}) \times 10^{-6}. \tag{3}$$

For $B \to K^*\ell^+\ell^-$ the significance is only 2.8σ, yielding a 90% confidence level (CL) upper limit of the branching fraction of

$$\mathcal{B}(B \to K^*\ell^+\ell^-) < 3.0 \times 10^{-6}. \tag{4}$$

Here, a ratio of $(B \to K^*e^+e^-)/(B \to K^*\mu^+\mu^-) = 1.2$ was assumed as predicted by the Ali *et al.* model [16]. Our $B \to K\ell^+\ell^-$ observation is consistent with a recent BELLE result [22] and most SM predictions but is larger than the recent Ali *et al.* prediction [16].

4 Search for $\mathbf{B} \to \rho\gamma$ and $\mathbf{B} \to \omega\gamma$

The electromagnetic penguin decays $B \to \rho\gamma$ and $B \to \omega\gamma$ are $b \to d$ transitions, which are suppressed with respect to $B \to K^*\gamma$ by $|V_{td}^2/V_{ts}^2|$. In SM branching fractions of the charged mode are predicted to lie in the range $\mathcal{B}(B^+ \to \rho^+\gamma) = 0.9 - 1.5 \times 10^{-6}$ [23]. Isospin symmetry and quark model relations yield a factor of two reduced branching fractions for the neutral modes. New Physics contributions may enhance the SM predictions.

In BABAR [25] we have searched for all three decay modes using a data sample of 77.8 fb^{-1} on the $\Upsilon(4S)$ resonance and 9.6 fb^{-1} 40 MeV below the $\Upsilon(4S)$ peak. Challenges in the analysis stem from a huge $q\bar{q}$ continuum background including initial state radiation (ISR). In addition, the ρ resonances are much broader than K^*'s and $B \to K^*\gamma$ events provide an additional source of background. Photon candidates with energies of 1.5 GeV $<$ $\mathrm{E}_\gamma^* < 3.5$ GeV, which are inconsistent with coming from a π^0 or η decay, are combined with ρ^+, ρ^0 and ω candidates. The latter are reconstructed from $\pi^+\pi^0$, $\pi^+\pi^-$ and three-pion combinations, using charged tracks that are inconsistent with a kaon hypothesis. The $\pi\pi$ (3π) invariant mass has to lie within a $520 - 1020$ MeV/c^2 ($759.6 - 805.6$ MeV/c^2) mass window and its momentum in the CM frame must satisfy $2.3 < \mathrm{p}_{\pi\pi}^* < 2.85$ GeV/c ($2.4 < \mathrm{p}_{3\pi}^* < 2.8$ GeV/c). A π^0 candidate must have a $\gamma\gamma$ invariant mass of $115 < \mathrm{m}_{\gamma\gamma} <$ 150 MeV/c^2. To improve momentum resolution we perform a kinematic fit with $m_{\gamma\gamma}$ constrained to the nominal π^0 mass. To suppress continuum and ISR backgrounds we use a neural network that combines different event shape variables, consisting of the energy flow in 18 cones around the photon momentum, the thrust angle θ_T, B decay angle θ_B, helicity angle θ_H, the ratio of second-to-zeroth Fox-Wolfram moments in a frame recoiling the photon, R_2', the net flavor content in the event, and the vertex separation of the candidate with respect to the other charged tracks. The output of the neural network is shown in Figure 8. Off-resonance data and $B \to D^-\pi^+$ data are used as a crosscheck. A maximum likelihood fit in the three-dimensional space $\Delta E^* - m_{ES} - m_\rho(m_\omega)$ is performed to extract signal yields. The procedure is crosschecked with a $B \to K^*\gamma$ sample. For $B \to K^{*0}$ (K^{*+})γ the fit yields 343.2 ± 21.0 (93.1 ± 12.6) events compared to expected yields of 332 ± 36 (105 ± 18) events, respectively.

The extracted signal yields of 4.8 ± 5.2 events for $B \to \rho^0\gamma$, 6.2 ± 5.5 events for $B \to \rho^+\gamma$, and 0.1 ± 2.3 events for $B \to \omega\gamma$ are consistent with background fluctuations. The efficiencies are 12.3%, 9.2% and 4.6%, respectively. Including systematic errors, which respectively increase from 11.8% to 13.4% and 17.3%, we obtain upper limits of branching fractions @ 90% CL of $\mathcal{B}(B^0 \to \rho^0\gamma) < 1.4 \times 10^{-6}$, $\mathcal{B}(B^+ \to \rho^+\gamma) < 2.3 \times 10^{-6}$ and $\mathcal{B}(B^0 \to \omega\gamma) < 1.2 \times 10^{-6}$. Combining these limits yields a ratio of $\mathcal{B}(B \to \rho\gamma)/\mathcal{B}(B \to K^*\gamma) < 0.047$ @ 90% CL. Using the parameterization [24]

$$\frac{\mathcal{B}(B \to \rho\gamma)}{\mathcal{B}(B \to K^*\gamma}) = \left|\frac{V_{td}}{V_{ts}}\right|^2 \left(\frac{1 - m_\rho^2/M_B^2}{1 - m_{K^*}^2/M_B^2}\right)^3 \zeta^2[1 + \Delta R] \tag{5}$$

with $\zeta = 0.07$ and $\Delta R = -0.25$ yields a ratio of $|V_{td}/V_{ts}| < 0.36$ @ 90% CL. This is still larger than the limit of $|V_{td}/V_{ts}| < 0.22$ @ 90% CL obtained from $B_s\bar{B}_s$ and $B_d\bar{B}_d$ mixing [12].

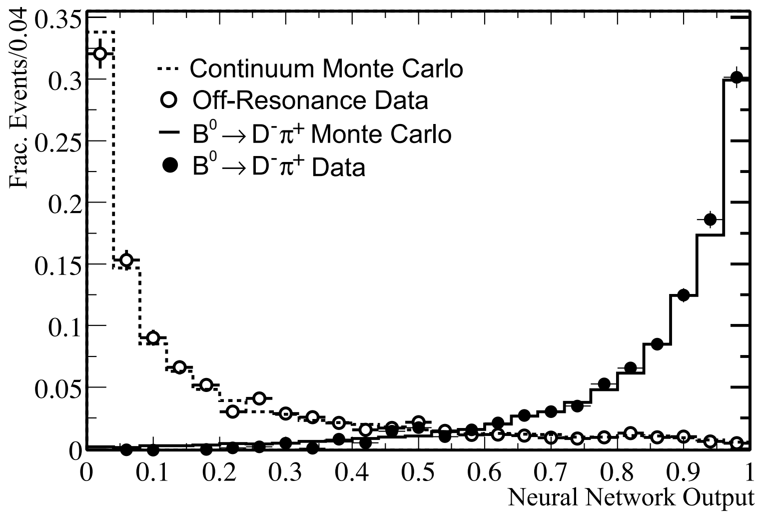

Figure 8: Output of a $B^0 \to \rho^0\gamma$ neural network for Monta Carlo simulated events and data control samples.

5 Search for $\mathbf{B^+ \to K^+\nu\bar{\nu}}$

The weak decay $B^+ \to K^+\nu\bar{\nu}$ proceeds via a Z^0 penguin loop or a weak box diagram. The diagrams are obtained from Figure 4 by interchanging ν's and charged leptons. Since higher-order QCD effects are smallest here in comparison to other electroweak penguin processes, these modes provide an excellent tool for searching for New Physics. In SM the branching fraction is predicted to be $\mathcal{B}(B^+ \to K^+\nu\bar{\nu}) = (3.8^{+1.2}_{-0.6}) \times 10^{-6}$. In BABAR [26] we have searched for this decay using a sample of 50.7 fb^{-1} [$(56.3 \pm 0.7) \times 10^6$ $B\bar{B}$ events] recorded at the $\Upsilon(4S)$. To beat down the enormous backgrounds from other B decays and $q\bar{q}$ continuum, one B meson is tagged via its decay, $B^- \to D^0\ell^-\bar{\nu}$, where the D^0 is reconstructed in $K^-\pi^+$, $K^-\pi^+\pi^0$ and $K^-\pi^+\pi^+\pi^-$ final states. Candidates are required to have exactly one charged kaon with a charge opposite to that of the lepton and a CM momentum of $p^* > 1.5$ GeV/c. The energy observed in the electromagnetic calorimeter after removing the decay products of the tagged B has to be $E^*_{\mathrm{cal}} < 0.5$ GeV. Signal candidates are selected in the $E^*_{cal} - \Delta m_D$ plane, where $\Delta m_D = m_D - m_D^{fit}$ is the difference between nominal and fitted D^0 mass of the tagged B. The signal region is defined as $E^*_{\mathrm{cal}} < 0.5$ GeV and $|\Delta m_D| < 3\sigma_D$. Two signal events are observed which are consistent with an expected background of 2.2 events. As a crosscheck between data and Monte Carlo simulation $B^- \to D^0\ell^-\bar{\nu} - B^+ \to \bar{D}^0\ell^+\nu$ double tagged events as well as data sidebands have been analyzed, yielding an efficiency correction by a factor of 0.92 ± 0.06. Since the overall selection efficiency is $\epsilon = 10.3\%$, we set an upper limit of the branching fraction of $\mathcal{B}(B^+ \to K^+\nu\bar{\nu}) < 9.4 \times 10^{-5}$ @ 90% CL. This limit is almost a factor of 30 above the SM prediction.

6 Search for $\mathbf{B \to e^+e^-, \mu^+\mu^-}$ and $\mathbf{e^\pm\mu^\mp}$

The decays $B \to \ell^+\ell^-$ are weak decays that are highly suppressed in SM, because they involve $b \to d$ transitions which require internal quark annihilation within the B meson and which are also helicity suppressed. For example, in SM branching fractions for e^+e^- and $\mu^+\mu^-$ final states are predicted to be $\mathcal{B}(B \to e^+e^-) = 1.9 \times 10^{-15}$ and $\mathcal{B}(B \to \mu^+\mu^-) = 8 \times 10^{-11}$ [28]. For $e^\pm\mu^\mp$ final states the branching fraction is tiny and non-zero only if ν's carry mass. New Physics processes arising, for example, from multi-higgs doublet models (MHDM), minimal supersymmetric models (MSSM) with large $\tan\beta$ values or $R-$parity-violating supersymmetry may enhance the branching fractions by several orders of magnitude [29]. In BABAR [27] we have searched for these modes using a data sample of 54.4 fb^{-1} [$(59.9 \pm 0.7) \times 10^6$ $B\bar{B}$ events] at the $\Upsilon(4S)$ resonance. Candidates are selected from events with two high-momentum leptons. Requirement on the event thrust of $|T| < 0.9$ and $|\cos\theta_T| < 0.84$ are used to suppress $q\bar{q}$ continuum. Signal yields are searched in the $\Delta E^* - m_{ES}$ plane. One candidate is observed in the e^+e^- channel while no events are seen in the $\mu^+\mu^-$ and $e^\pm\mu^\mp$ final states. These yields are consistent with residual backgrounds of 0.60 ± 0.24 e^+e^- events, 0.49 ± 0.19 $\mu^+\mu^-$ events and 0.51 ± 0.17 $e^\pm\mu^\mp$ events. While backgrounds from $c\bar{c}$ continuum events contribute to all three modes, π/μ misidentification contributes to both $\mu^+\mu^-$ and $e^\pm\mu^\mp$ modes and $\gamma\gamma$ processes to both e^+e^- and $e^\pm\mu^\mp$ modes. With respective efficiencies of 19.3%, 18.8% and 18.3% for the three modes branching fraction upper limits have been derived, yielding $\mathcal{B}(B \to e^+e^-) < 3.3 \times 10^{-7}$, $\mathcal{B}(B \to \mu^+\mu^-) < 2.0 \times 10^{-7}$, and $\mathcal{B}(B \to e^\pm\mu^\mp) < 2.1 \times 10^{-7}$ @ 90% CL.

7 Conclusion and Outlook

The precision of V_{ub} measurements in exclusive charmless semileptonic decays is presently limited by theoretical uncertainties arising in the calculations of hadronic form factors. Since these uncertainties $(15\% - 20\%)$ are non-probabilistic, they need to be kept separate from experimental errors. For example, in global fits of the CKM matrix [31] they require special treatments, since they should not be added in quadrature with statistical and systematic errors. Unquenched lattice gauge calculations are expected to predict these form factors some day with pure probabilistic errors. Thus, in the near future reduced theoretical uncertainties of order 10% are expected only from an analysis of inclusive charmless semileptonic decays in the low m_{had} and high q^2 plane [4].

The present data samples of 10^8 $B\bar{B}$ events provides sensitivities to observe decay modes with branching fractions at the 10^{-6} level. Both, BELLE and BABAR have observed first signals in $B \to K^+\ell^+\ell^-$ with branching fractions $(0.75^{+0.25}_{-0.21} \pm 0.09) \times 10^{-6}$ and $(0.78^{+0.24+0.11}_{-0.20-0.18}) \times 10^{-6}$, respectively. In addition, BELLE has reported first signals in the inclusive decays $B \to X_s\ell^+\ell^-$ [32]. For $B \to \rho\ (\omega)\gamma$ the branching fraction upper limits are approaching the SM predictions. For the summer conferences BABAR also presented preliminary results for $B \to X_s\gamma$. Using a data sample of $(59.6 \pm 0.7) \times 10^6$ $B\bar{B}$ events we measure a branching fraction of $\mathcal{B}(B \to X_s\gamma) = (3.88 \pm 0.36 \pm 0.37^{+0.43}_{-0.23}) \times 10^{-4}$ [30]. This value though consistent with previous measurements is about 15% higher and agrees with recent SM predictions [33]. For $B^+ \to K^+\nu\bar{\nu}$ our 90% CL upper limit lies a factor of 30 above the predicted SM branching fraction, while for $B^0 \to \ell^+\ell^-$ our upper limits are are several orders of magnitude above the SM predictions.

Our data sample will be doubled in the next year. This statistical increase should be sufficient to observe the electroweak penguin mode $B \to K^*\ell^+\ell^-$ and increase the precision on $B \to K\ell^+\ell^-$. According to our planned luminosity increases we expect to accumulate a data sample of 0.5 ab^{-1} in BABAR by the end of 2005. Such a large data sample looks rather promising for discovering $B \to \rho\gamma$ and $B \to \omega\gamma$ modes. This sample is also suitable to observe CP asymmetries in $B \to K^*\gamma$ and $B \to X_s\gamma$ at a few % level. The observation of $B \to K^{(*)}\nu\bar{\nu}$ decays has to await a super B factory reaching luminosities of 10^{36}cm^{-2}s^{-1}, since these decays cannot be measured in hadron colliders due to large backgrounds. Unless New Physics processes enhance $B \to \ell^+\ell^-$ decays considerably, these modes may be difficult to observe even in a hadron machine or a super B factory. Thus, the next few years will be exciting with respect to gaining new insights on rare B decays.

8 Acknowledgment

I would thank the BABAR collaboration for providing this opportunity for me to give this talk. I would like to thank L. Wilden, A. Ryd and M. Convery for assistance. This work was supported by the Norwegian Reasearch Council.

References

[1] B. Aubert *et al.* (BABAR collaboration), SLAC-PUB-9293, 7pp submitted to Phys. Rev. Lett. (2002).

[2] J. Bartelt *et al.* (CLEO collaboration), Phys. Rev. Lett. **71**, 4111 (1993).

[3] J.P. Alexander *et al.* (CLEO collaboration), Phys. Rev. Lett. **77**, 5000 (1996); B.H. Behrens *et al.* (CLEO collaboration), Phys. Rev. **D61**, 052001 (2000).

[4] C.W. Bauer, Z. Ligeti and M.E. Luke, Phys. Rev. **D64**, 113004 (2001).

[5] B. Aubert *et al.* (BABAR collaboration), SLAC-PUB-9305, 19 pp (Jul 2002).

[6] D. Scora and N. Isgur, CEBAF preprint No. CEBAF-TH-94-14 (1994).

[7] L. Del Debbio *et al.* (UKQCD collaboration), Phys. Lett. **B416**, 392 (1998).

[8] M. Beyer and D. Melikhov, Phys. Lett. **B436**, 433 (1998).

[9] P. Ball and V.M. Braun, Phys. Rev. **D58**, 094016 (1998).

[10] Z. Ligeti and M.B. Wise, Phys. Rev. **D53**, 4937 (1996).

[11] G.C. Fox and S. Wolfram, Phys. Rev. **Lett. 41**, 1581 (1978).

[12] K. Hagiwara *et al.* (Particle Data Group) Phys. Rev. **D66**, 010001 (2002).

[13] A. Bornheim *et al.* (CLEO collaboration), Phys. Rev. Lett. **88**, 231803 (2002).

[14] B. Aubert *et al.* (BABAR collaboration), SLAC-PUB-9282, 17 pp (Jul 2002).

[15] V_{ub} working group, http://battagl.home.cern.ch/battagl/vub/vub.html; R. Barate *et al.* (ALEPH collaboration), Eur. Phys. J. **C6**, 555 (1999); P. Abreu *et al.* (DELPHI collaboration), Phys. Lett. bf B478, 14 (2000); M. Acciarri *et al.* (L3 collaboration), Phys.Lett. **B436**, 174 (1998); G. Abbiendi *et al.* (OPAL collaboration), Eur. Phys. J. **C21**, 399 (2002).

[16] A. Ali *et al.*, Phys. Rev. **D66**, 034002 (2002).

[17] P. Colangelo *et al.*, Phys. Rev. **D53**, 3672 (1996); D. Melikhov *et al.*, Phys. Rev. **D57**, 6814 (1998); A. Ali *et al.*, Phys. Rev. **D61**, 074024 (2000); M. Benecke *et al.*, Nucl. Phys. B612, 25 (2001).

[18] B. Aubert *et al.* (BABAR collaboration), SLAC-PUB-9323, 33 pp (Jul 2002).

[19] R.A. Fisher, Ann. Eugenics **7** (1936).

[20] T. Skwarnicki, DESY internal report No DESY-F31-86-02 (1986); T. Skwarnicki *et al.* (Crystal Ball collaboration) Phys. Rev Lett. **58**, 972 (1987).

[21] H. Albrecht *et al.* (ARGUS collaboration), Phys. Lett. **B241**, 278 (1990).

[22] K. Abe *et al.* (BELLE collaboration), Phys. Rev. Lett. **83**, 021801 (2002).

[23] M. Benecke *et al.*, Nucl. Phys. **B612**, 25 (2001); S.W. Bosch and G. Buchalla, Nucl. Phys. **B621**, 459 (2002).

[24] A. Ali and A. Y. Parkhamenko, Eur. Phys. J. C23, 89 (2001).

[25] B. Aubert *et al.* (BABAR collaboration), SLAC-PUB-9319, 17 pp (Jul 2002).

[26] B. Aubert *et al.* (BABAR collaboration), SLAC-PUB-9309, 15 pp (Jul 2002).

[27] B. Aubert *et al.* (BABAR collaboration), SLAC-PUB-9313, 16 pp (Jul 2002).

[28] A. Ali *et al.*, ECFA-93-151,C93/03/26 report, 155 (1993).

[29] J.L. Hewett *et al.*, Phys. Rev. **D39**, 259 (1989); X.G. He *et al.*, Phys. Rev. **D38**, 814 (1988); Y. Nir and D. Silverman, Phys. Rev. **D42**, 1477 (1990); M. Gronau and D. London, Phys. Rev. **D55**, 2845 (1997).

[30] B. Aubert *et al.* (BABAR collaboration), SLAC-PUB-9301, 16 pp (Jul 2002).

[31] G. Dubois-Felsmann *et al.*, CALT 68-2396 preprint at ICHEP02 (ABS959), 14 pp (2002).

[32] K. Abe *et al.* (BELLE collaboration), BELLE preprint 2002-28, KEK-preprint-83, 10 pp submitted to Phys. Rev. Lett. (2002).

[33] P.Gambino and M. Misiak, Nucl. Phys. **B611**, 338 (2001) A.J. Buras *et al.*, Nucl. Phys. **B631**, 219 (2002).